J. Electrochem. Sci. Eng. **2(1)** (2012) 1-18; doi: **10.5599/jese.2011.0006**

Open Access : : ISSN 1847-9286
www.jESE-online.org

Original scientific paper

Inhibition of corrosion of carbon steel by heptane sulphonic acid – Zn^{2+} system

C. MARY ANBARASI and SUSAI RAJENDRAN*✉

PG Department of Chemistry, Jayaraj Annapackiam College for Women, Periyakulam-625601, India, E-mail: anbuc_m@yahoo.co.in
**Corrosion Research Centre, PG and Research Department of Chemistry, GTN Arts College, Dindigul-624005 and Department of Chemistry, RVS School of Engineering and Technology, Dindigul-624005, India*

✉Corresponding author: E-mail: susairajendran@gmail.com; Tel: +91-0451-2424114; Fax: +91-0451-2424114

Received: May 6, 2011; Revised: October 11, 2011; Published: March 22, 2012

Abstract

Corrosion inhibition of carbon steel in dam water by sodium heptane sulphonate (SHS) and zinc ion system was investigated using weight loss and potentiodynamic polarization methods. Results of weight loss method indicated that inhibition efficiency (IE) increased as the inhibitor concentration increased. A synergistic effect existed between SHS and Zn^{2+}. The influence of sodium potassium tartrate (SPT) on the IE of the SHS-Zn^{2+} system was evaluated. As the immersion period increased, the IE decreased. Polarization study revealed that SHS-Zn^{2+} system functioned as a cathodic inhibitor. AC impedance spectra revealed that a protective film was formed on the metal surface. The nature of the metal surface was analyzed by FTIR spectra, SEM and AFM analyses.

Keywords

Carbon steel; Corrosion; Electrochemical techniques; FTIR; SEM; AFM.

Introduction

Natural water is frequently used in cooling systems. Cooling water circuits may present several problems. Corrosion, scale and fouling by microorganisms can appear when natural water is used as thermal fluid. These problems can occur jointly, reducing the thermal efficiency of the circuits with significant economic repercussions. To eliminate or to reduce these problems, water used in cooling circuits is treated with inhibitive formulations. Inhibitors are generally used in these processes to control metal dissolution.

Organic compounds are recognized as effective inhibitors of the corrosion of many metals and alloys. The efficiency of an organic compound as a corrosion inhibitor is closely associated with the chemical adsorption [1-5]. Most of these organic compounds contain nitrogen, sulphur, oxygen and multiple bonds in the molecules, which are adsorbed on the metal surface and the organic compound [6, 7]. Much interest has been devoted to organic inhibitors such as polyethylene glycols [8], 1,2,3 benzotriazole [9], 2 mercaptobenzimidazole [10], ethoxylated fatty acids [11] and meta substituted aniline-N-sallicylidenes [12]. Protecting efficiency was also found to be improved with increasing length of alkyl chain and with the increase of the organic compound concentration [13]. A survey of the available literature reveals that the corrosion inhibition of 2-naphthalenesulfonic acid, 2,7-naphthalenedisulfonic acid, and 2-naphthol-3,6-disulfonic acid on Armco-iron electrode in sulfuric acid has been investigated by Vračar and Dražić [14]. The inhibition efficiency changes with the number of functional groups substituted on benzene ring and increases with the concentration of inhibitors [14]. The inhibitory action of 2-mercaptobenzoxazol, 2-mercaptobenzimidazole, N-cetylpyridiniumbromide, and propargylbenzene-sulphonate on the corrosion of carbon steel in acid media has also been studied by Prakash Rajesh Kumar Singh and Ranju Kumar [15]. The corrosion inhibitors are used to reduce corrosion damage in sub-surface equipments in oil well field. The corrosion inhibition activity was studied by gravimetric and potentiostatic polarization methods in the presence of 20% HCl [15]. Manickavasagam *et al*. [16] reported the corrosion inhibition of poly-(styrene sulphonic acid)-doped polyaniline on carbon steel in acid media. The polymer acts as an anodic inhibitor. The adsorption of the compound on the metal surface obeys Temkin's adsorption isotherm [16]. Aliev [17] has described the influence of salts of alkyl phenol sulphonic acid on the corrosion of ST3 steel. The protective effect increases with temperature. The investigated compounds inhibit corrosion of ST3 steel as a result of chemical adsorption [17]. Shakkthivel and Vasudevan [18] have studied acrylic acid-diphenylamine sulphonic acid copolymer threshold inhibitor for sulphate and carbonate scales in cooling water systems. The results showed that the polymer acts as a very good antiscaling inhibitor both in the carbonate and sulphate brines. Copolymer of acrylic acid-diphenylamine sulphonic acid can be used safely in cooling water industries [18].

The present work is undertaken to evaluate the inhibition efficiency (*IE*) of sodium heptane sulphonate (SHS) – Zn^{2+} system in controlling corrosion of carbon steel immersed in dam water in the absence or presence of Zn^{2+} by weight loss method; to investigate the influence of immersion period on the IE of the system; to analyze the protective film by FTIR spectra, fluorescence spectra, Scanning Electron Microscope (SEM), and Atomic Force Microscope (AFM); and to propose the mechanism of corrosion inhibition based on the above results.

Experimental

Preparation of the Specimen

Carbon steel specimens of size 1.0 cm × 4.0 cm × 0.2 cm and chemical composition 0.026 % sulphur, 0.06 % phosphorous, 0.4 % manganese, 0.1 % carbon, and the rest iron were polished to a mirror finish, degreased with trichloroethylene, and used for the weight loss method and surface examination studies.

Weight-loss Method

Carbon steel specimens were immersed in 100 ml of the Sothuparai dam water in Tamil Nadu, India, containing various concentrations of the inhibitor sodium heptane sulphonate (Scheme 1) in

(cc) BY

the absence and presence of Zn^{2+} for 3 days. The weights of the specimens before and after the immersion were determined using a Digital Balance (Model AUY 220 SHIMADZU). The corrosion products were cleaned with Clarke's solution prepared by dissolving 20 g of Sb_2O_3 and 50 g of $SnCl_2$ in one litre of concentrated HCl of specific gravity 1.9 [19]. The corrosion IE was then calculated using the equation

$$IE = 100\ [1-(W_2/W_1)]\ \% \quad (1)$$

where W_1 is the weight loss value in the absence of inhibitor and W_2 is the weight loss value in the presence of inhibitor. Corrosion rate (in mils per year) was calculated using the formula

$$CR = 534\ W / DAT \quad (2)$$

W = weight loss in milligrams
D = density of specimen = 7.87 g cm^{-3}
A = area of specimen = 10.4 cm^2
T = exposure time in hours = 72 hrs.

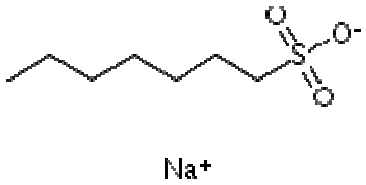

Scheme 1. *Molecular structure of sodium heptane sulphonate*

Surface Examination Study

The carbon steel specimens were immersed in various test solutions for a period of one day. After one day, the specimens were taken out and dried. The nature of the film formed on the surface of the metal specimen was analyzed by various surface analysis techniques.

Fourier Transforms Infrared Spectra

These spectra were recorded in a Perkin-Elmer-1600 spectrophotometer using KBr pellets. The FTIR spectrum of the protective film was recorded by carefully removing the film, mixing it with KBr and making the pellet.

UV visible absorbance spectra and fluorescence spectra

The instrument UV Spetord S-100 Analytic Jena was used for recording UV visible absorbance spectra. Fluorescence spectra were recorded in a Glaxo F-6300 Spectro fluorimeter.

Scanning Electron Microscopic Studies (SEM)

The carbon steel samples immersed in blank solution and in the inhibitor solution for a period of one day were removed, rinsed with double distilled water, dried and observed under a scanning electron microscope to examine the surface morphology. The surface morphology measurements of carbon steel were examined using JEOL MODEL6390 computer-controlled scanning electron microscope.

Atomic Force Microscopy Characterization (AFM)

The carbon steel specimen immersed in blank and in the inhibitor solution for a period of one day were removed, rinsed with double distilled water, dried and subjected to the surface examination. Atomic force microscopy (Veeco dinnova model) was used to observe the samples'

surface in tapping mode, using cantilever with linear tips. The scanning area in the images was 5 µm × 5 µm and the scan rate was 0.6 Hz s^{-1}.

Potentiodynamic Polarization

Polarization studies were carried out with a CHI-electrochemical work station with impedance model 660A. It was provided with IR compensation facility. A three-electrode cell assembly was used. The working electrode was carbon steel. An SCE was the reference electrode. Platinum was the counter electrode. From polarization studies, corrosion parameters such as corrosion potential (E_{corr}), corrosion current (I_{corr}), Tafel slopes anodic = b_a, and cathodic = b_c were calculated and linear polarization study (*LPR*) was done. The scan rate (v) was 0.01 V s^{-1}. Hold time at E_f was 0 s and quiet time t_q was 2 s.

AC Impedance Spectra

The instrument used for polarization study was also used to record AC impedance spectra. The cell set up was also the same. The real part (Z') and imaginary part (Z'') of the cell impedance were measured in ohms at various frequencies. Values of charge transfer resistance (R_t) and the double layer capacitance (C_{dl}) were calculated. AC impedance spectra were recorded with initial $E_{(v)}$ = 0 V, high frequency limit was 1×10^5 Hz, low frequency limit was 1 Hz, amplitude = 0.005 V and quiet time t_q = 2 s.

Determination of the Biocidal Efficiency

The biocidal efficiency of the system was determined using a Zobell medium and calculating the number of colony forming unit per ml using a bacterial colony counter. The biocidal efficiency of sodium dodecyl sulphate (SDS) was determined. Various concentrations of SDS, namely 50 ppm, 100 ppm, 150 ppm, 200 ppm, and 250 ppm, were added to the formulation consisting of the inhibitor system. Polished and degreased carbon steel specimens in duplicate were immersed in these environments for a period of three days. After three days, one ml of each test solution from the above environment was pipetted out into sterile Petri dishes each containing about 20 ml of the sterilized Zobell medium. The Petri dishes were then kept in a sterilized environment inside the laminar flow system fabricated for 48 hours. The total viable hydrotropic bacterial colonies were counted using a bacterial colony counter. The biocidal efficiencies of the formulation consisting of the inhibitor in the presence of various concentrations of SDS were also calculated.

Results and Discussion

Weight-loss Study

The physicochemical parameters of dam water are given in Table 1. The corrosion inhibition efficiencies of sodium 1-heptane sulphonate (SHS)-Zn^{2+} systems and the corresponding corrosion rates (mils per year) are given in Table 2.

The inhibition efficiencies of SHS-Zn^{2+} systems are given in Table 2. It was found that the *IE* increases as the concentration of SHS increases. As the concentration of Zn^{2+} increases, *IE* also increases. A synergistic effect exists between SHS and $Zn^{2+.}$ For example, 250 ppm of SHS has 28 % *IE*. 30 ppm of Zn^{2+} has 21% *IE*. However, interestingly, the formulation consisting of 250 ppm of SHS and 30 ppm of Zn^{2+} has 75% *IE*. This is the mixture of inhibitors that shows better inhibition efficiency than the individual inhibitors [20].

(cc) BY

Table 1. *Water Analysis (Sothuparai dam water, Tamil Nadu, India)*

Parameter	Result
Appearance	Brownish
Total dissolved solids	100 ppm
Electrical conductivity	140 µS cm^{-1}
pH	8.25
Total hardness as $CaCO_3$	50 ppm
Calcium	10 ppm
Magnesium	6 ppm
Iron	1.2 ppm
Nitrate	10 ppm
Chloride	10 ppm
Sulphate	2 ppm

Table 2. *The corrosion inhibition efficiencies and the corresponding corrosion rates of SHS-Zn^{2+} systems*

c_{SHS} / ppm	c_{Zn2+} / ppm					
	0		15		30	
	IE / %	*CR* / mpy	*IE* / %	*CR* / mpy	*IE* / %	*CR* / mpy
0	-	4.4384	12	3.9058	21	2.5063
50	12	3.9058	33	2.9737	47	2.3523
100	17	3.6839	31	3.0625	4748	2.3079
150	21	3.5063	36	2.8406	53	2.0860
200	22	3.4620	39	2.7074	65	1.5534
250	28	3.1956	41	2.6187	75	1.1096

Synergism Parameter (S_I)

Synergism parameters are indications of synergistic effect existing between inhibitors [21, 22]. S_I value is found to be greater than the one indicating synergistic effect existing between Zn^{2+} of concentrations 15ppm and 30 ppm and various concentrations of SHS. The results are given in Table 3.

$$S_I = (1-I_{1+2})/(1-I'_{1+2}) \quad [3]$$

where $I_{1+2} = (I_1+I_2)-(I_1 \times I_2)$
I_1 = surface coverage of inhibitor (SHS)
I_2 = surface coverage of inhibitor (Zn^{2+})
I'_{1+2} = combined surface coverage of inhibitors (SHS) and (Zn^{2+})
Surface coverage = (*IE* /100) / %.
I_2 for Zn^{2+} (15 ppm) = 0.12 and I_2 for Zn^{2+} (30 ppm) = 0.21

Table 3. *Synergism parameter (S_I).*

c_{SHS} / ppm	I_1	SHS-Zn^{2+}(15 ppm) I'_{1+2}	S_I	SHS-Zn^{2+}(30 ppm) I'_{1+2}	S_I
50	0.12	0.33	1.1558	0.47	1.3117
100	0.17	0.31	1.058	0.48	1.2610
150	0.21	0.36	1.086	0.53	1.3279
200	0.22	0.39	1.125	0.65	1.7606
250	0.28	0.41	1.073	0.75	2.2752

Analysis of Variance (F- Test)

F-test was used to investigate whether the synergistic effect existing between two inhibitors is statistically significant [23, 24]. If F-value was above 5.32 for 1,8 degrees of freedom, the synergistic effect proved to be statistically significant. If it was below 5.32 for 1, 8 degrees of freedom, it was statistically insignificant at a 0.05 level of significance. The results are given in Table 4.

Table 4. *Analysis of Variance (F- Test)*

c_{Zn2+} /ppm	Source of variances	Sum of squares	Degrees of freedom	Mean square	F-value	*p* value
15	between within	128 210	1 8	128 26.25	4.8762	< 0.05
30	between within	706.88 725.20	1 8	706.88 90.65	7.7979	>0.05

The obtained F- value of 4.8762 for 15 ppm of Zn^{2+} was not statistically significant. Therefore, it was concluded that the influence of 15 ppm of Zn^{2+} on the inhibition efficiencies of various concentrations of SHS was not statistically significant.

The obtained F- value of 7.7979 for 30 ppm of Zn^{2+} was statistically significant. Therefore, it was concluded that the influence of 30 ppm of Zn^{2+} on the inhibition efficiencies of various concentrations of SHS was statistically significant.

Influence of Immersion Period on the IE of SHS (250 ppm) - Zn^{2+} (30 ppm) System

The influence of immersion period on *IE* of SHS (250 ppm) - Zn^{2+} (30 ppm) is shown in Table 5.

Table 5. *Influence of immersion period on the IE of SHS (250 ppm) - Zn^{2+} (30 ppm) system.*

System	Immersion period, days				
	1	3	5	7	10
Dam water (DW) *CR* / mpy	7.8431	4.4384	6.8400	4.0914	4.4327
DW+SHS (250 ppm)+Zn^{2+}(30 ppm) *CR* /mpy	1.4902	1.1096	2.1888	1.6365	2.3050
IE / %	81	75	68	60	48

It was found that, as the immersion period increases, the inhibition efficiency decreases. This may be due to the fact that, as the period of immersion increases, the protective film Fe^{2+}- SHS complex formed on the metal surface is broken by the continuous attack of other ions present in

(cc) BY

the environment; hence, the IE decreases as the immersion period increases. A similar behavior was observed in the corrosion prevention of carbon steel by methyl orange [25].

Influence of pH on the IE of SHS (250 ppm) - Zn^{2+} (30 ppm) System

The influence of pH (addition of H_2SO_4 or addition of NaOH) on the *IE* of SHS -Zn^{2+} system is given in Table 6.

Table6. *Influence of pH on the IE of SHS (250 ppm) - Zn^{2+} (30 ppm) system; Immersion period three days*

System	pH				
	3	5	7	9	11
Dam water (DW) *CR* / mpy	6.1535	5.9589	4.4384	4.8036	3.3443
DW+SHS (250 ppm)+Zn^{2+}(30 ppm) *CR* /mpy	2.8306	2.2644	1.1096	0.9127	0.4682
IE / %	54	62	75	81	86

All the reactions involved in corrosion process can be classified into a few general reactions [26]. The anodic reaction in every corrosion reaction is the oxidation of a metal to its ion.

$$M \rightarrow M^{n+} + ne^- \quad (4)$$

The number of electrons produced is the valence of the ion.

There are several different cathodic reactions that are frequently encountered in metallic corrosion. The most common are:

Hydrogen evolution $2H^+ + 2e^- \rightarrow H_2$ (5)

Oxygen reduction (acid solution) $O_2 + 4H^+ + 4e^- \rightarrow 2H_2O$ (6)

Oxygen reduction (neutral or basic solution) $O_2 + 2H_2O + 4e^- \rightarrow 4OH^-$ (7)

In the present study, it was observed that the *IE* decreased when the pH of the solution was lowered (pH=5 and pH=3). This is acidic medium and hence the anodic reaction is dissolution of metal (equation 4) and the cathodic reactions are evolution of hydrogen and oxygen reduction (equations 5 and 6). Because of the release of hydrogen gas from the metal surface, blistering of the protective film takes place and the protective film formed is broken [21].

When the pH is increased (alkaline medium), oxygen is reduced to hydroxide ion (equation 7). The Zn^{2+} ion combines with OH^- ion to form $Zn(OH)_2$ as an insoluble film on the metal surface. Thus, cathodic reaction is controlled and hence the corrosion potential shifts to more negative direction.

Influence of Sodium Potassium Tartrate (SPT) on the IE of SHS (50 ppm) - Zn^{2+} (15 ppm) System

The *IE* and *CR* of carbon steel immersed in solutions containing SHS (50 ppm) - Zn^{2+} (15 ppm) and various concentrations of SPT are presented in Table 7.

Table 7. *Influence of sodium potassium tartrate (SPT) on the IE of SHS (50 ppm) - Zn^{2+} (15 ppm) system*

c_{SHS} / ppm	c_{Zn2+}/ ppm	c_{SPT} / ppm	*CR* / mpy	*IE* / %
0	0	0	4.4384	-
50	15	0	2.9737	33
50	15	50	0.3551	92
50	15	100	0.2663	94
50	15	150	0.0888	98
50	15	200	0.5326	88
50	15	250	0.6214	86

It is noted that for SPT, *IE* increases up to the concentration of 150 ppm and then it decreases. As the concentration of inhibitors (SPT) increases, more of the inhibitors are transported towards the metal surface through the formation of Zn^{2+}-inhibitor complex. On the metal surface, Zn^{2+}-inhibitor complex is converted into Fe^{2+}- inhibitor complex. This complex is insoluble, stable, and more compact and, therefore, *IE* increases up to 150 ppm concentration. On further increasing the concentration of the inhibitors, the complex formed on the metal surface goes into solution. Thus, the *IE* decreases. Another reason may be that when more inhibitors are added, the Zn^{2+}- inhibitor complex formed is precipitated in the bulk of the solution. Also, the inhibitors are not transported towards the metal surface; hence, the *IE* decreases. Similar observations have been made by Rajendran et al. while studying the inhibition efficiency of Henna extract [27] and also by Arockia Selvi *et al*. [28] who investigated the inhibition efficiency of diethylenetriamine penta-methylene-phosphonic acid-Zn^{2+} system.

Biocidal Efficiency of SDS - SHS (250 ppm)- Zn^{2+} (30 ppm) System

Table 8. *Influence of biocide (SDS) on SHS (250 ppm)- Zn^{2+} (30 ppm) system*

c_{SHS} / ppm	c_{Zn2+}/ ppm	c_{SDS} / ppm	Colony forming unit	Biocidal efficiency, %
0	0	0	26×10^4	-
0	0	150	18×10^4	30
250	30	50	59×10^3	77
250	30	100	22×10^3	91
250	30	150	14×10^3	94
250	30	200	43×10^2	98
250	30	250	nill	100

The biocidal nature of SDS (an anionic surfactant) has also been studied [29]. The inhibitor system that offered the best corrosion inhibition efficiency was selected. Biocidal efficiency of SDS at various concentrations on the best system in dam water is determined. It is interesting to note that the SHS (250 ppm)- Zn^{2+} (30 ppm) system has some biocidal efficiency (BE).

In Table 8, 150 ppm of SDS alone has 30 % BE. When 50 ppm of SDS is added to the SHS (250 ppm)- Zn^{2+} (30 ppm) system, BE increases from 30% to 77%. On increasing the concentration of SDS from 50 ppm to 100 ppm, 150 ppm, 200 ppm, BE continues to increase and 100% BE is achieved when the concentration of SDS is 250 ppm.

(cc) BY

Analysis of polarization curves

The potentiodynamic polarization curves of carbon steel immersed in various test solutions are shown in Fig.1. The corrosion parameters are given in Table 9.

***Table 9**. Corrosion parameters of carbon steel immersed in dam water in the presence and absence of inhibitor obtained by polarization method*

c_{SHS} / ppm	$c_{Zn^{2+}}$/ ppm	E_{corr} / mV *vs* SCE	I_{corr} / A cm^{-2}	b_a / mV dec^{-1}	b_c / mV dec^{-1}	*LPR* / Ω cm^2
0	0	-494	2.66×10^{-6}	166	203	2.053×10^{4}
250	30	-573	4.96×10^{-7}	181	152	7.701×10^{4}

When carbon steel is immersed in dam water, the corrosion potential, E_{corr}, is -494 mV *vs* SCE. The formulation consisting of 250 ppm SHS + 30 ppm Zn^{2+} shifts the corrosion potential to -573 mV *vs* SCE. This suggests that the cathodic reaction is controlled predominantly. The corrosion current value and linear polarization resistance (*LPR*) value for dam water are $I_{corr} = 2.66\times10^{-6}$ A cm^{-2} and *LPR* = 2.053×10^{4} Ω cm^2.

For the formulation of SHS (250 ppm) + Zn^{2+} (30 ppm), the corrosion current value (I_{corr}) has decreased to 4.96×10^{-7} A cm^{-2}, and the LPR value has increased to 7.701×10^{4} Ω cm^2. This indicates that a protective film is formed on the metal surface. When a protective film is formed on the metal surface, *LPR* value increases and corrosion current value decreases. The fact that the *LPR* value increases with decrease in corrosion current indicates that inhibition of corrosion takes place by the formation of a protective film. There is an increase in the value of anodic Tafel slope. Similar observations have been reported by Joseph Rathish *et al.* [30] while studying the corrosion behavior of metals in artificial sweat; Yesu Thangam *et al.* [31] while studying inhibition of corrosion of carbon steel in a dam water by sodium molybdate-Zn^{2+} system, and also by Agnesia Kanimozhi and Rajendran [29] while studying the corrosion inhibition sodium tungstate-Zn^{2+}-ATMP system.

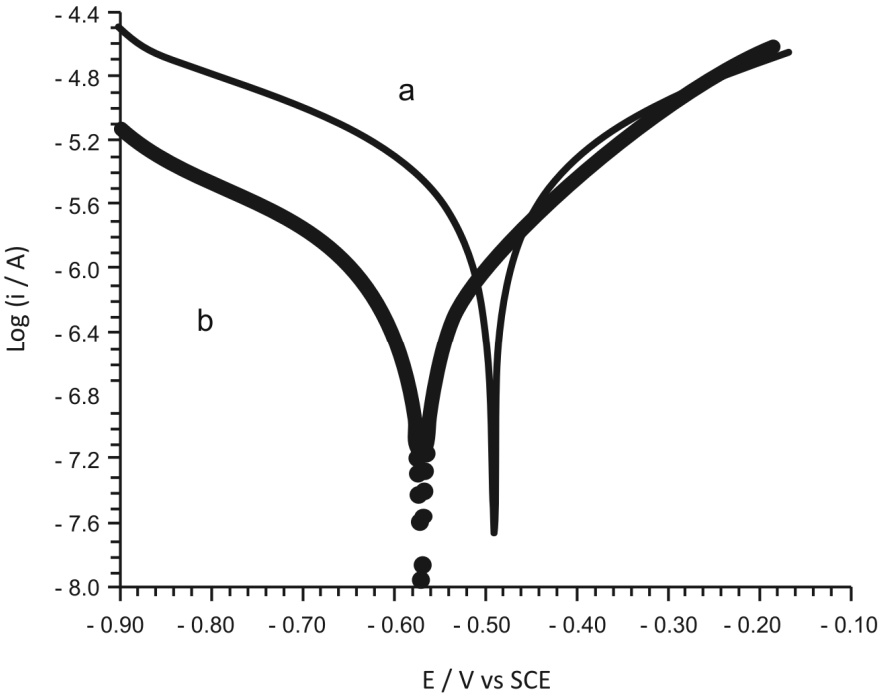

***Fig 1.** Polarization curves of carbon steel immersed in various test solutions **a**) dam water **b**) dam water containing 250 ppm of SHS and 30 ppm of Zn^{2+}*

Analysis of AC impedance spectra

AC impedance spectra have been used to detect the formation of a film on the metal surface. If a protective film is formed, the charge transfer resistance (R_t) increases and double layer capacitance (C_{dl}) value decreases [32, 33]. The AC impedance spectra of carbon steel immersed in various solutions are shown in Fig. 2.

***Table 10**. Impedance parameters of carbon steel in dam water in the presence and absence of inhibitor obtained by AC impedance method*

c_{SHS} / ppm	c_{Zn2+}/ ppm	R_t / Ω cm^2	C_{dl} / F cm^{-2}	log (Z / Ω)
0	0	1.084×10^4	8.24×10^{-10}	4.062
250	30	1.8837×10^4	4.72×10^{-10}	4.276

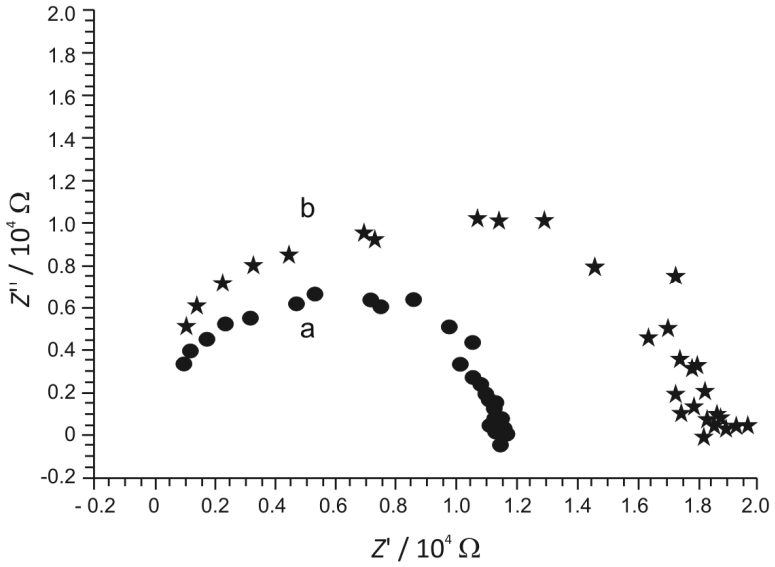

***Fig. 2.** AC impedance spectra of carbon steel immersed in various test solutions **a**) dam water **b**) dam water containing 250 ppm of SHS and 30 ppm of Zn^{2+}*

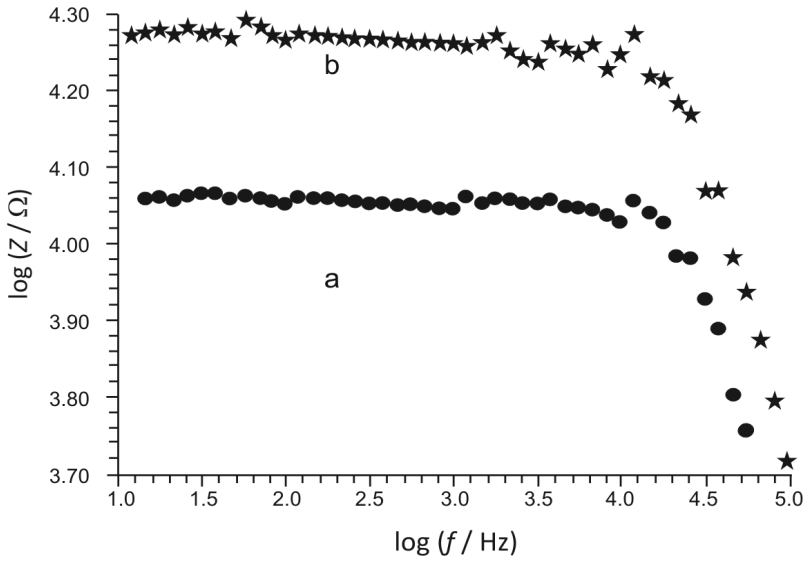

***Fig. 3.** AC impedance spectra of carbon steel immersed in various test solutions. (frequency Bode plots) **a)** dam water **b**) dam water containing 250 ppm of SHS and 30 ppm of Zn^{2+}*

(cc) BY

The AC impedance parameters, *i.e.,* charge transfer resistance (R_t) and double layer capacitance (C_{dl}), are given in Table 10. When carbon steel is immersed in dam water, R_t value is 1.084×10^4 Ω cm^2 and C_{dl} value is 8.24×10^{-10} F cm^{-2}. When SHS and Zn^{2+} are added to dam water, R_t value increases from 1.084×10^4 Ω cm^2 to 1.8837×10^4 Ω cm^2 and the C_{dl} decreases from 8.24×10^{-10} F cm^{-2} to 2.13×10^{-10}. This suggests that a protective film is formed on the surface of the metal. This is further supported by the increase in impedance value log*Z* from 4.062 Ω to 4.276 Ω (Fig. 3). This accounts for the very high IE of SHS–Zn^{2+} system.

Analysis of FTIR spectra

Earlier researchers have confirmed that FTIR spectrometer is a powerful instrument that can be used to determine the type of bonding for organic inhibitors adsorbed on the metal surface [34]. FTIR spectra were used to analyze the protective film formed on metal surface. FTIR spectrum of pure SHS is given in Fig. 4a. The FTIR spectrum of the film formed on the metal surface after immersion in the dam water for 3 days containing 250 ppm of SHS and 30 ppm of Zn^{2+} is shown in Fig. 4b. The S=O stretching frequency has decreased from 1193 cm^{-1} to 1118 cm^{-1}. This indicates that the oxygen atom of S=O group has coordinated with Fe^{2+} formed on the metal surface, resulting in the formation of Fe^{2+}-SHS complex on the anodic sites of the metal surface. The peak at 1399 cm^{-1} is due to Zn-O stretching. The stretching frequency due to –OH appears at 3398 cm^{-1}. Therefore, it is concluded that Zn $(OH)_2$ is formed on cathodic sites of the metal surface [35].

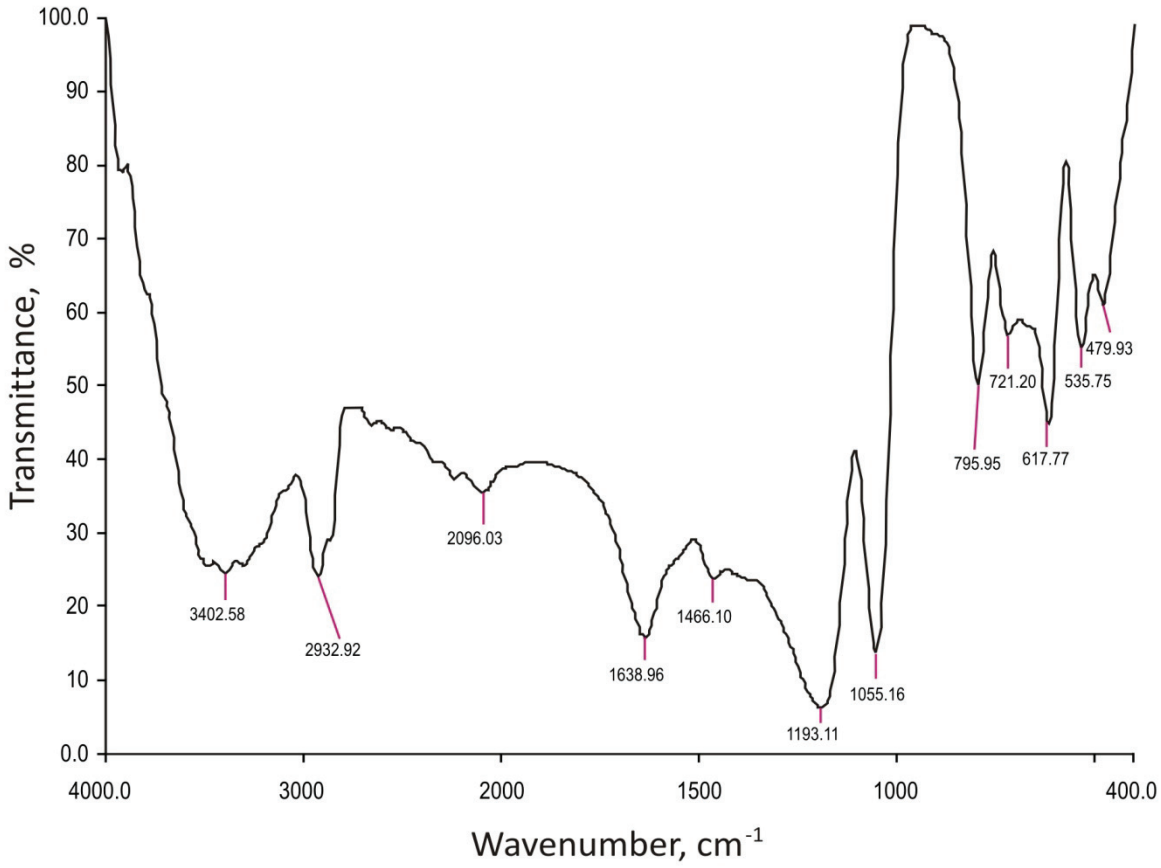

Fig. 4a. *FTIR spectrum of pure sodium heptane sulphonate*

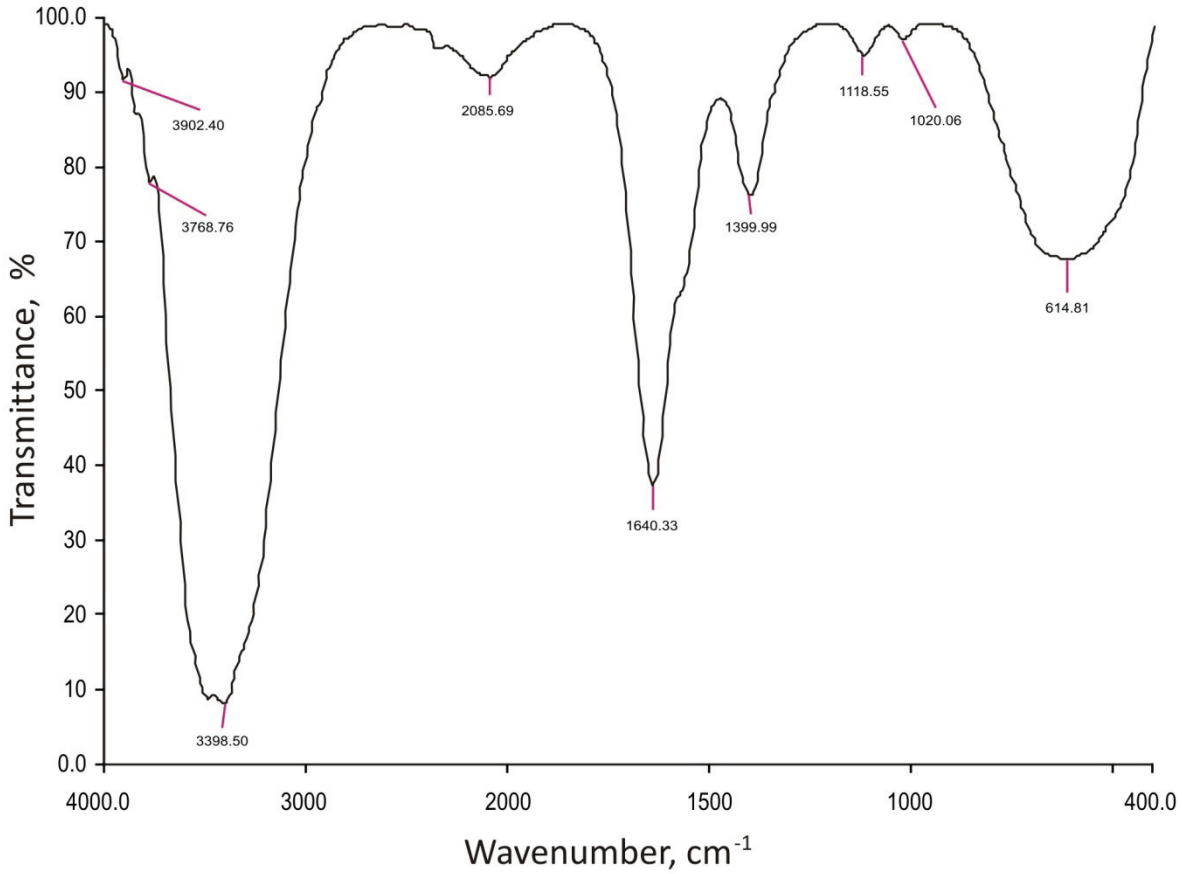

***Fig. 4b**. FTIR spectrum of film formed on metal surface after immersion in dam water containing 250 ppm of SHS -30 ppm of Zn^{2+}*

UV-visible absorbance spectra and fluorescence spectra.

UV-visible absorption spectra and fluorescence spectra can be used to confirm the protective film formed on the metal surface [36, 37].

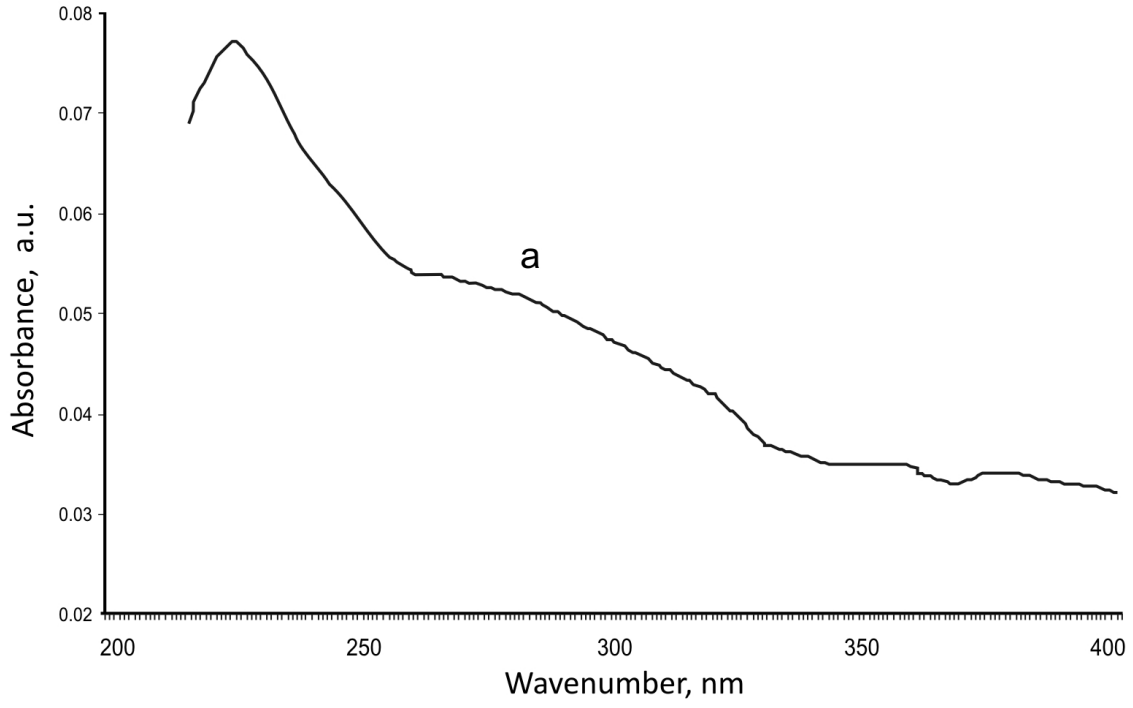

***Fig. 5a.** UV visible absorption spectra of SHS solution*

(cc) BY

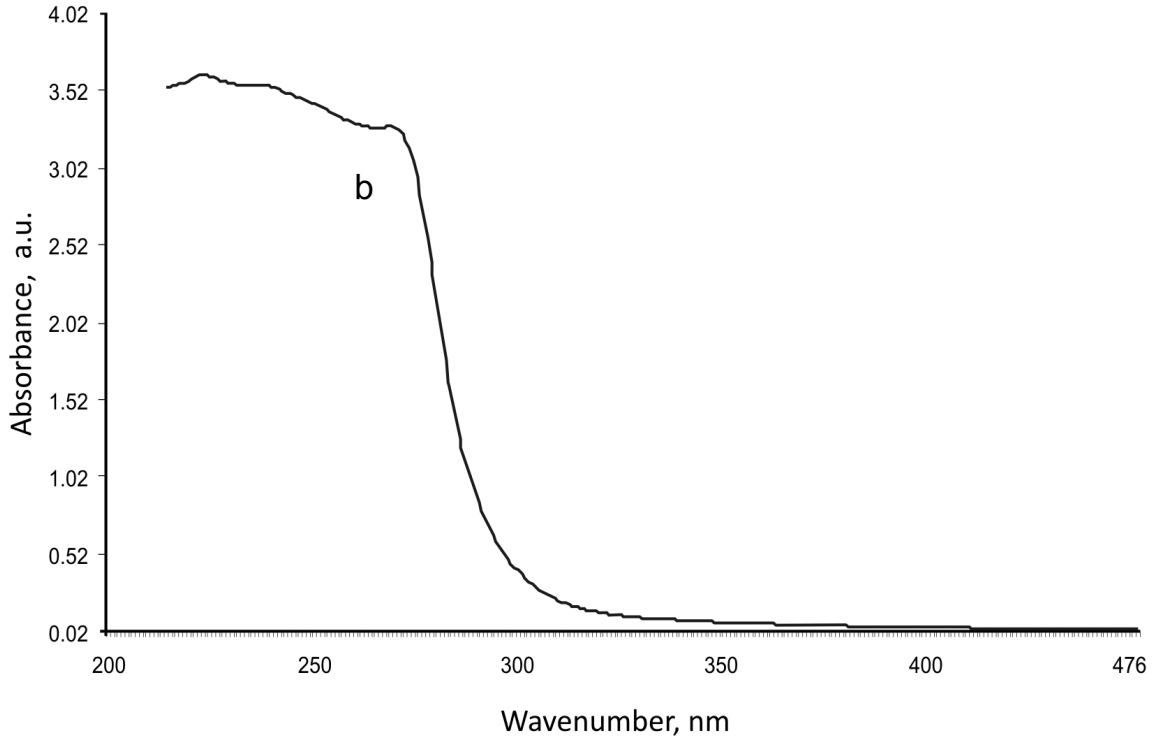

Fig. 5b. *UV visible absorption spectra of SHS+Fe^{2+} solution*

UV-visible absorption spectrum of an aqueous solution of sodium heptane sulphonate (SHS) is shown in Fig. 5 curve (a). The peak appears at 226 (0.077) nm (the peak intensity is given in parentheses). The corresponding emission spectrum (λ_{ex} = 226 nm) is shown in Fig. 6 curve (a). Peaks appear at 396 (3.71), 450 (1.41), and 505 (1.91) nm (the peak intensities are given in parentheses). Fe^{2+}–SHS complex in solution was prepared by mixing SHS solution and Fe^{2+} ion (as $FeSO_4 \cdot 7H_2O + H_2O$ freshly prepared). Its UV-visible absorption spectrum is shown in Fig. 5 curve (b). Peaks appear at 226 (3.62), 242 (3.56) and 278 (3.29) nm. The corresponding emission spectrum (λ_{ex} = 226 nm) is shown in Fig. 6 curve (b). Peaks appear at 397 (4.35) and 510 (2.30) nm. These peaks correspond to Fe^{2+} - SHS complex.

The emission spectrum (λ_{ex} = 226 nm) of the film formed on the carbon steel metal surface after immersion in the solution containing 30 ppm of Zn^{2+} and 250 ppm of SHS is shown in Fig. 6 curve (c). Peaks appear at 395 (3.88) and 511 (1.79) nm. These peaks correspond to Fe^{2+}-SHS complex. Thus, fluorescence spectral study leads to the conclusion that protective film consists of Fe^{2+}-SHS complex formed on the metal surface.

SEM Analysis of Metal Surface

The SEM image of ×500 magnification of carbon steel specimen immersed in dam water for one day in the absence and presence of inhibitor system are shown in Figs.7b and 7c, respectively.

The SEM micrographs of polished carbon steel surface (control) in Fig. 7a shows the smooth surface of the metal. This implies the absence of any corrosion product formed on the metal surface.

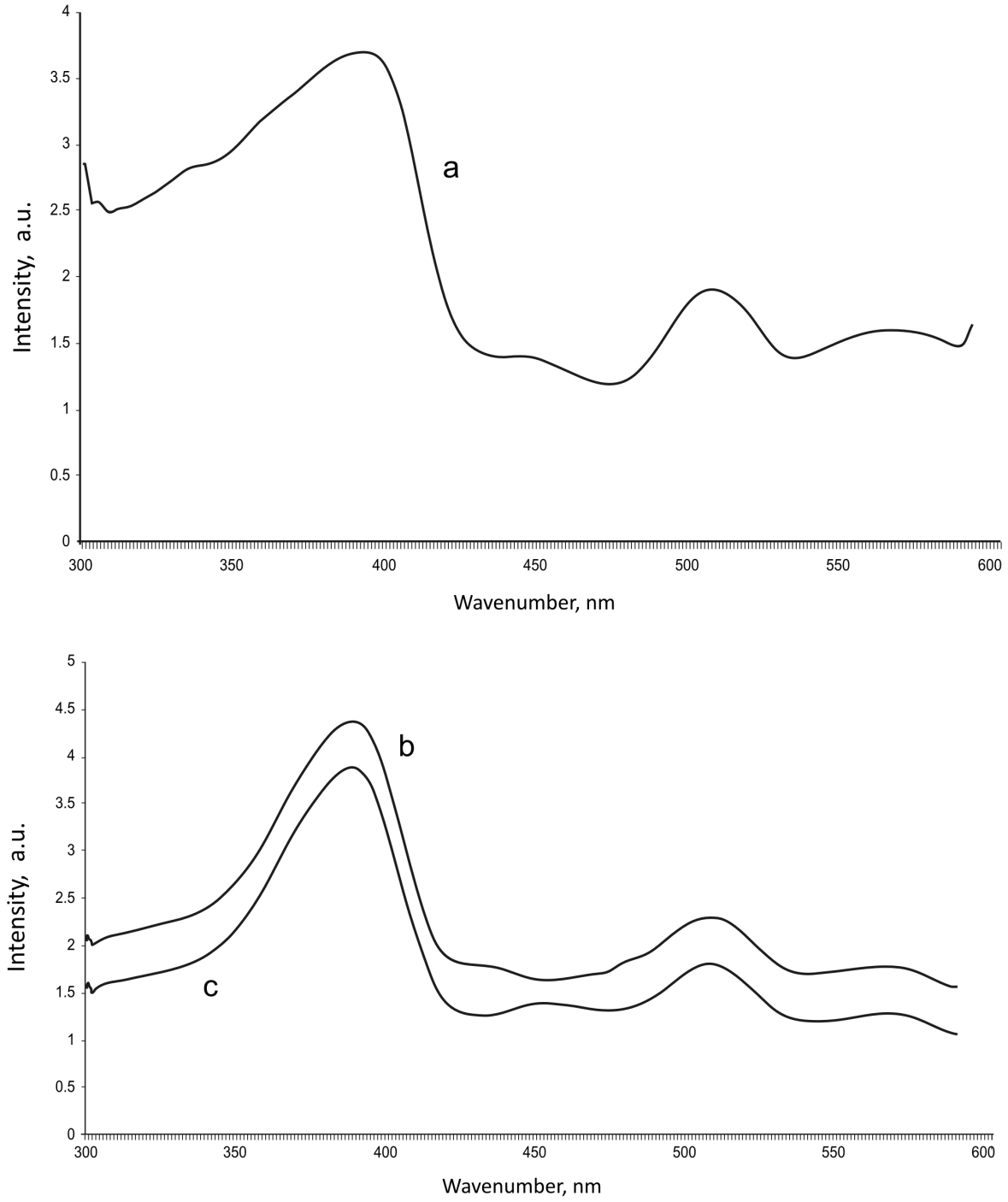

Fig. 6: *Fluorescence Spectra* ***a)*** *SHS solution;* ***b)*** *SHS+Fe^{2+} solution ,****c)*** *film formed on metal surface after immersion in solution containing dam water + 250 ppm of SHS and 30 ppm of Zn^{2+}*

The SEM micrographs of carbon steel surface immersed in dam water in Fig. 7b show the roughness of the metal surface, which indicates the corrosion of carbon steel in dam water. Fig. 7c indicates that, in the presence of 250 ppm of SHS and 30 ppm of Zn^{2+} mixture in dam water, the surface coverage increases, which in turn results in the formation of insoluble complex on the surface of the metal (SHS-Zn^{2+} inhibitor complex) and the surface is covered by a thin layer of inhibitors, which control the dissolution of carbon steel. Such results were reported earlier [38].

(cc) BY

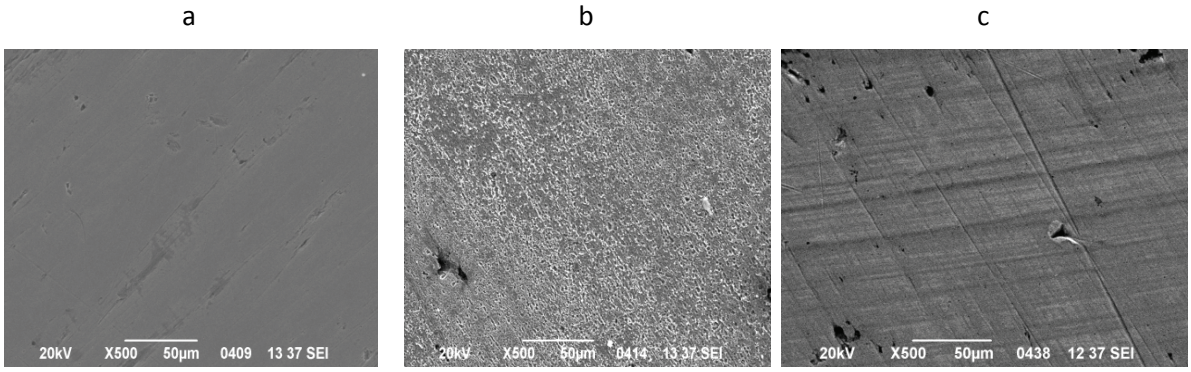

Fig. 7. *SEM micrographs (magnification-×500) of* ***a)*** *polished carbon steel (control) -* ***b)*** *carbon steel immersed in dam water*
c) *carbon steel immersed in dam water containing 250 ppm of SHS and 30 ppm of* Zn^{2+}

Atomic Force Microscopy Characterization

AFM is a powerful technique to investigative the surface morphology at nano- to micro-scale and has become a new choice to study the influence of inhibitor on the generation and progress of the corrosion at the metal/solution interface [38-40]. The three dimensional (3D) AFM morphologies and the AFM cross-sectional profile for polished carbon steel surface (reference sample), carbon steel surface immersed in dam water (blank sample), and carbon steel surface immersed in dam water containing the formulation of 250 ppm of SHS and 30 ppm of Zn^{2+} are shown as Figs. 8a and 8d; 8b and 8e; and 8c and 8f, respectively.

Root– Mean-Square Roughness, Average Roughness and Peak-to-Valley Value

AFM image analysis was performed to obtain the average roughness, R_a (the average deviation of all points roughness profile from a mean line over the evaluation length), root-mean-square roughness, R_q (the average of the measured height deviations taken within the evaluation length and measured from the mean line), and the maximum peak-to-valley, *P-V*, height values (largest single peak-to-valley height in five adjoining sampling heights) [38]. Table 11 is a summary of R_q, R_a, *P-V* values for carbon steel surface immersed in different environment.

Figs. 8a and 8d displays the surface topography of un-corroded metal surface. The value of R_q, R_a and *P-V* height for the polished carbon steel surface (reference sample) are 4.3 nm, 3.41 nm, and 35.28 nm respectively. The slight roughness observed on the polished carbon steel surface is due to atmospheric corrosion.

Figs. 8b and 8e displays the corroded metal surface with few pits in the absence of the inhibitor immersed in dam water. The R_q, R_a and *P-V* height values for the carbon steel surface are 31.9 nm, 24.9 nm, and 420.3 nm, respectively. These data suggest that carbon steel surface immersed in dam water has a greater surface roughness than the polished metal surface, which shows that the unprotected carbon steel surface is rougher due to the corrosion of the carbon steel in dam water environment.

Figs. 8c and 8f displays the steel surface after immersion in dam water containing 250 ppm of SHS and 30 ppm of Zn^{2+}. The R_q, R_a and *P-V* height values for the carbon steel surface are 1.17 nm, 0.89 nm, and 10.37 nm, respectively. The R_q, R_a and *P-V* height values are considerably lower in the inhibited environment compared to the uninhibited environment. These parameters confirm that the surface is smoother. The smoothness of the surface is due to the formation of a compact protective film of Fe^{2+}- SHS complex and $Zn(OH)_2$ on the metal surface, thereby inhibiting the corrosion of carbon steel [38].

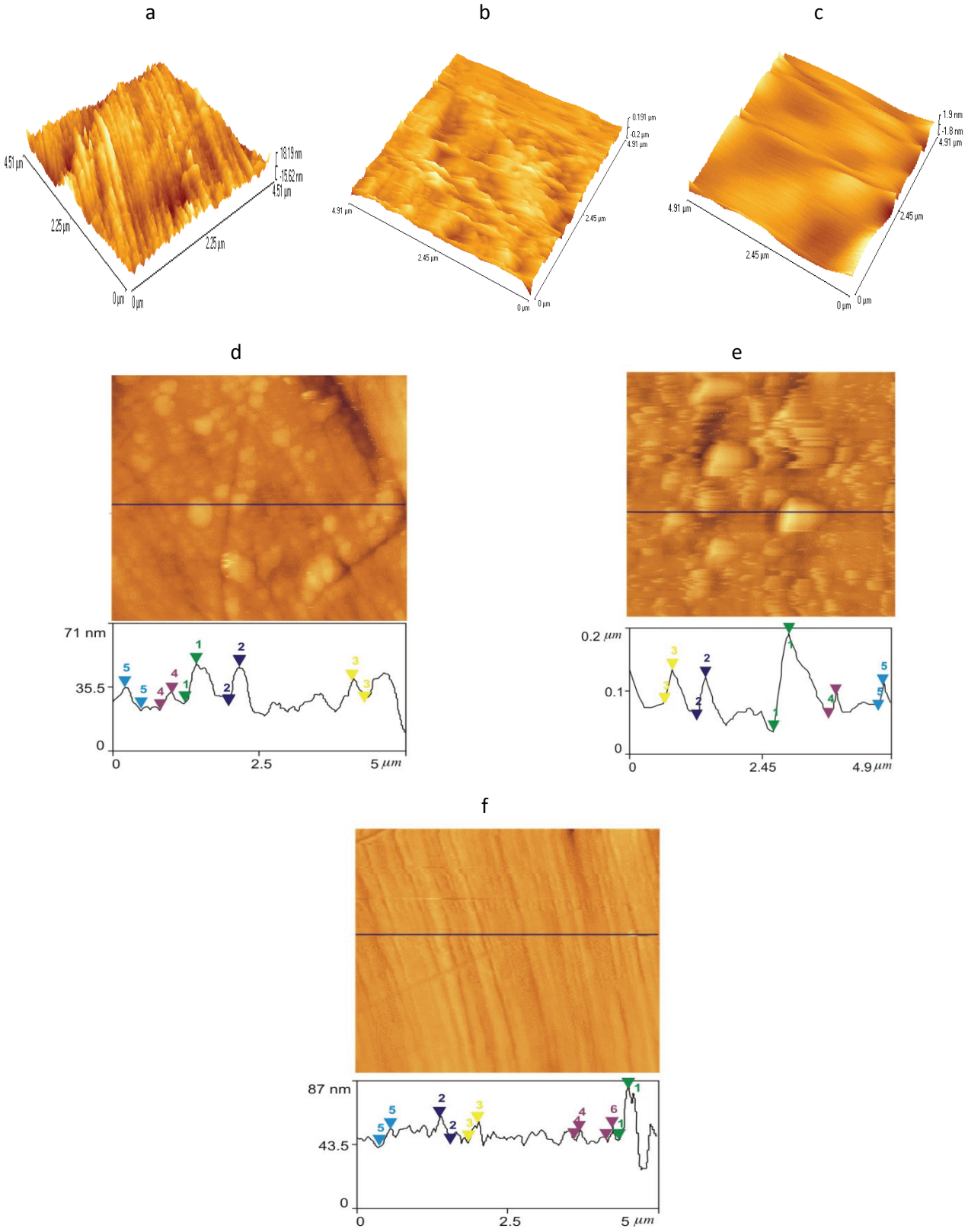

Fig. 8. *Three dimensional AFM images of:* ***a)*** *polished carbon steel (control);* ***b)*** *carbon steel immersed in dam water (blank);* ***c)*** *carbon steel immersed in dam water containing SHS (250 ppm) + Zn^{2+} (30ppm); AFM cross-sectional images of the surface of:* ***d)*** *polished carbon steel (control);* ***e)*** *carbon steel immersed in dam water (blank);* ***f)*** *carbon steel immersed in dam water containing SHS (250 ppm) + Zn^{2+} (30ppm).*

(cc) BY

Table 11. *AFM data for carbon steel surface immersed in inhibited and uninhibited environment*

Samples	R_q / nm	R_a /nm	Maximum peak-to-valley height, nm
Polished carbon steel	4.33	3.41	35.28
Carbon steel immersed in dam water (blank)	31.9	24.9	420.3
Carbon steel immersed in dam water + SHS (250ppm) + Zn^{2+}(30ppm)	1.17	0.89	10.37

Mechanism of corrosion inhibition

From the above discussion, a mechanism may be proposed for the corrosion inhibition of carbon steel immersed in dam water containing 250 ppm SHS and 30 ppm Zn^{2+} system.

When the formulation consists of 250 ppm of SHS and 30 ppm of Zn^{2+} in dam water, there is formation of SHS – Zn^{2+} complex in solution.

When carbon steel is immersed in this solution SHS– Zn^{2+} complex diffuses from the bulk of the solution towards the metal surface.

SHS Zn^{2+} complex is converted into SHS Fe^{2+} complex on the anodic sites of the metal surface with the release of Zn^{2+} ion.

$$Zn^{2+}SHS + Fe^{2+} \rightarrow Fe^{2+}SHS + Zn^{2+} \quad (8)$$

The released Zn^{2+} combines with OH^- to form $Zn(OH)_2$ on the cathodic sites of the metal surface

$$Zn^{2+} + 2\ OH^- \rightarrow Zn(OH)_2\downarrow \quad (9)$$

Thus the protective film consists of SHS Fe^{2+} complex and $Zn(OH)_2$.

This accounts for the synergistic effect of SHS Zn^{2+} system.

Conclusions

The present study leads to the following conclusions:

The inhibition efficiency (IE) of SHS in controlling corrosion of carbon steel immersed in dam water in the absence and in presence of Zn^{2+} has been evaluated by weight loss method. The formulation consisting of 250 ppm SHS and 30 ppm Zn^{2+} has 75% IE. As the immersion period increases, the IE decreases. Polarization study reveals that SHS – Zn^{2+} system functions as a cathodic inhibitor. AC impedance spectra reveal that a protective film is formed on the metal surface. FTIR spectra reveal that the protective film consists of Fe^{2+} SHS complex and $Zn(OH)_2$.

Acknowledgements: *The authors are thankful to their respective management and University Grants Commission, New Delhi.*

References

[1] A. Spinelli, R.S. Gonclaves, *Corros.Sci.* **30** (1990) 1235-1246
[2] W.X. Oliver, R.S.Gonclaves, *J. Braz .Chem. Soc.* **3** (1992) 92-94
[3] Z.B. Vendrame, R.S. Gonclaves, *J. Braz .Chem. Soc.***9** (1998) 441-448
[4] L.D. Melloo, R.S. Gonclaves, *Corros.Sci.* **43** (2001) 457-470
[5] A.M. Lucho, R.S. Gonclaves, D.S. Azambuja, *Corros.Sci.* **44** (2002) 467-479.
[6] S. Martinez, I. Stern, *Appl. Surf. Science* **199** (2002) 83-89
[7] S. Manov, A.M. Lamazouere, L. Aries, *Corros.Sci.* **42** (2000) 1235-1248
[8] J. Dobryszycki, S. Biallozor, *Corros.Sci.* **43** (2001) 1309-1319
[9] K. Aramaki, *Corros.Sci.* **43** (2001) 1985-2000

[10] L. Wang, J.X. Pu, H.C. Luo, *Corros.Sci.* **45** (2003) 677-683
[11] E.E.F. El-Sherbin, S.M.A. Wahaab, M. Deyab, *Mat. Chem. Phys.* **89** (2005) 83-191
[12] J.D. Talti, M.N. Desai, N.K. Shah, *Mat. Chem. Phys.* **93** (2005) 54-64
[13] A. Srhiri, M.Etman, F.Dabosi, *Electrochim. Acta* **41** (1996) 429-437
[14] Lj.M. Vracar , D.M .Drazic, *Corros.Sci.* **44** (2002) 1669-1680
[15] D. Prakash Rajesh Kumar Singh, R.Kumar, *Indian J. Chem.Techn.* **13** (2006) 555-560
[16] R. Manickavasagam, K. Jeya Karthik, M. Paramasivam, S. Venkatakrishna Iyer, *Anti- Corros. Methods M.,* **49** (2002) 19-26
[17] T.A. Aliev, *Mat. Sci.* **44** (2008) 69-74
[18] P. Shakkthivel , T. Vasudevan, *Desalination* **197** (2006) 179-189
[19] G. Wranglen, Chapman & Hall, London (1985) 236
[20] T. Umamathi, J. A. Selvi, S.Agnesia Kanimozhi, S. Rajendran, A. John Amalraj, *Indian J. Chem.Techn.* **15** (2008) 560-565
[21] S. Rajendran, S. Shanmugapriya, T. Rajalakshmi , A.J. Amalraj, *Corrosion* **61** (2005) 685-692.
[22] K.A.Radha, R.Vimala, B.Narayanasamy, J.A.Selvi , S.Rajendran, *Chem. Eng. Commun.* **195** (2008) 352-366
[23] S. Rajendran, A. Raji, J. A. Selvi, A. Rosaly , S. Thangasamy, *J.Mater. Ed.* **29** (2007) 245-258
[24] S. Rajendran, A. Raji, J. Arockia Selvi, A. Rosaly, Thangasamy, *Edutracks.* **6** (2007)30-33
[25] J. Sathiyabama, S. Rajendran, J. A. Selvi, A. J. Amalraj, *Indian J. Chem.Techn*. **15** (2008)462-466
[26] M.G. Fontana, Corrosion Engineering, TATA McGraw-Hill Publishing Company Limited, New Delhi, Third edition, 2006, p.16
[27] S. Rajendrran, M. Agasta, R. B. Devi, B. Sh.Devi, K. Rajam, J. Jeyasundari, *Zastita Materijala.* **50** (2009) 77-84
[28] J. A. Selvi, S.Rajendran, J. Jeyasundari, *Zastita Materijala.* **50** (2009) 91-98
[29] S. A.Kanimozhi, S. Rajendran, *Arab. J. Sci. Eng.* **34** (2009) 37-47
[30] R.J. Rathish, S. Rajendran, J.L. Christy J, *et al. Open Corrosion Journal* **3** (2010) 38-44
[31] Y.Y. Thangam, M.Kalanithi, C.M.Anbarasi, S.Rajendran, *Arab. J. Sci. Eng.* **34** (2009) 49-60
[32] J. Sathiyabama, S. Rajendran, J. A.Selvi, *B. Electrochem.* **22** (2006) 363-370
[33] S. Rajendran M. Manivannan, J.W. Sahayaraj, J.A. Selvi, J. Sathiyabama, A. Amalraj, N. Palaniswamy, *Trans. SAEST.* **41** (2006) 63-67
[34] A. Lalitha, S. Ramesh, S. Rajeswari, *Electrochim. Acta* **51** (2005) 47–55
[35] R. M. Silverstein, F. X. Webster: *Spectrometric Identification of Organic Compounds*, VI Edition, Wiley Student Editon, 2007 p-108
[36] S. Rajendran, B.V. Apparao, N. Palaniswamy, *B. Electrochem* **12** (1996) 15-19
[37] S. Rajendran, S. M.Reenkala, N. Anthony, R. Ramaraj, *Corros. Sci.* **44** (2002) 2243-2252
[38] B. Sherine, A. J.A. Nasser, S. Rajendran, *Int. J. Eng. Sci. Technol.* **24** (2010) 341-357
[39] A.K. Singh, M.A. Quraishi, *Corros.Sci.* **53** (2011) 1288-1297
[40] B. Wang, M.Du, J. Zhang, C.J. Gao, *Corros.Sci.* **53** (2011) 353-361

© 2012 by the authors; licensee IAPC, Zagreb, Croatia. This article is an open-access article distributed under the terms and conditions of the Creative Commons Attribution license (http://creativecommons.org/licenses/by/3.0/) (cc) BY

(cc) BY